Adsorbate order-disorder effects on recombinative thermal desorption: Equivalence between dynamic Monte Carlo simulations and self-consistent cluster approximations

Sieghard Weinketz and G. G. Cabrera

Citation: The Journal of Chemical Physics **106**, 1620 (1997); doi: 10.1063/1.473229

View online: http://dx.doi.org/10.1063/1.473229

View Table of Contents: http://scitation.aip.org/content/aip/journal/jcp/106/4?ver=pdfcov

Published by the AIP Publishing

Adsorbate order-disorder effects on recombinative thermal desorption: Equivalence between dynamic Monte Carlo simulations and self-consistent cluster approximations

Sieghard Weinketz and G. G. Cabrera
Instituto de Física ''Gleb Wataghin,'' Universidade Estadual de Campinas (UNICAMP), Caixa Postal 6165, 13083-970 Campinas, Brazil

(Received 11 July 1996; accepted 8 October 1996)

The thermally activated desorption of dissociated diatomic species from a metallic surface is described as a lattice-gas problem on a square lattice with nearest- and next-nearest neighbor interactions between the adsorbates and investigated within dynamic Monte Carlo simulations. In the limit of fast diffusion with respect to desorption, it can be shown that the desorption rate depends directly on the local order induced by the interactions within the adsorbate layer. Therefore, by employing an appropriate quasi-equilibrium cluster approximation for the local order (beyond the quasi-chemical approximation), a differential equation can be derived that depends on self-consistently calculated structure forms, reproducing quantitatively the temperature-programmed desorption spectra simulated with the Monte Carlo procedure. In this way it can be shown that the time evolution obtained from the dynamic Monte Carlo algorithm is indeed ''correct,'' and on the other hand, that it can be successfully substituted by a ''cheaper'' cluster approximation.
 [S0021-9606(97)01503-1]

I. INTRODUCTION

Time-dependent (or dynamical) Monte Carlo simulations have been widely used in the simulation of thermal desorption processes of simple molecules from metallic surfaces,[1–6] as a practical way to work out the corresponding lattice-gas models. In this way it has been possible to obtain an interrelationship between the adsorbate overlayer structure, its energetics and the desorption kinetics as a function of temperature and surface coverage,[1] considering the local processes of desorption, diffusion and (eventually) adsorption, with their proper local neighborhood dependencies. The kinetic lattice-gas model[7] is justified since the adsorbed species are located around well-defined equilibrium positions at the surface sites,[8,9] treating the thermally activated local processes as stochastic transitions.

In the dynamic Monte Carlo procedure of Fichthorn and Weinberg[10] the time evolution of a given system is obtained from the sum of its microscopic processes in terms of a heterogeneous Poisson process[11] (an equivalent algorithm was previously devised by Gillespie,[12] derived from a correspondence to the master equation formalism). As applied to the simulation of temperature-programmed desorption processes, the procedure will obtain time increments between successive events as a function of the total transition rate of all the desorption and diffusion events,[6] handled on the same footing, or just of desorption events,[4,5] where diffusion is treated as a ''thermalization'' process due to its much smaller time scale.[13,14]

Analytical treatments for the lattice-gas desorption problem are also possible within appropriate statistical approximations,[7,15] and a comparison between the two approaches should be sought. Therefore, even though Monte Carlo methods are easy to implement and produce reliable results, they are rather ''costly'' in terms of computing effort, and often carry fluctuation errors and problems due to insufficient thermalization. Analytical approximations, on the other hand, will be much faster and provide smoother results, but they are often unreliable or too difficult to calculate. Thus, whenever a quantitative comparison between the two approaches can be attained, a much higher confidence on both solutions will be also achieved.

In this work we present a dynamic Monte Carlo procedure for temperature-programmed desorption (TPD) of dissociated diatomic species on a square lattice, considering nearest and next-nearest neighbor interactions between the adsorbates. The lattice-gas model and the dynamic Monte Carlo procedure are presented in Section II, where the diffusion ''rescaling'' problem is also discussed, showing the direct dependence of the desorption kinetics on the (quasi-equilibrium) local order as derived from the stochastic model. This allows a direct comparison to the local order obtained from an appropriate minimum free-energy approximation as the C_2 approximation of the cluster variation method, and thus to the development of a dynamical approximation for the desorption kinetics, as presented in Section III. The numerical results for the adsorbate nearest and next-nearest neighbor correlation functions, showing the equivalence between both approaches, are presented in Section IV, particularly discussing the case where the adsorbate layer undergoes an order-disorder transition with a consequent vanishing of one the correlation functions. The equivalence between both methods for TPD spectra is shown in Section V, and the final remarks are presented in Section VI.

II. RECOMBINATIVE DESORPTION MODEL AND MONTE CARLO ALGORITHM

The metallic surface is represented by a square lattice with periodic boundary conditions, with $N_s = 100 \times 100$ sites,

 0021-9606/97/106(4)/1620/8/$10.00

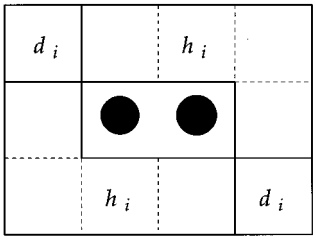

FIG. 1. Partition of the immediate neighborhood to the central pair of adsorbates in terms of the h_i and d_i clusters.

each one being either empty or occupied by an adsorbate. N_A is the total number of adsorbates, and the surface coverage is defined by $\theta = N_A/N_s$. The system dynamics is defined by two classes of local processes: pair desorption and diffusion, characterized by transition rates with an Arrhenius temperature dependence and activation energies dependent on the local environment.

Pair desorption will occur when two nearest neighboring (lateral) sites are both occupied, leaving the sites empty, with a transition rate

$$r_{des}^{ij} = \nu_{des} \exp[-(E_{des} - i\Delta_l - j\Delta_d)/k_B T], \tag{1}$$

where ν_{des} is the desorption pre-exponential factor, E_{des} is the activation energy in the limit of zero coverage, k_B is the Boltzmann constant and T is the absolute temperature. Δ_l and Δ_d are, respectively, the nearest (lateral) and next-nearest (diagonal) interaction energies (repulsive energies positively defined), and i and j the corresponding numbers of occupied nearest and next-nearest neighbors for the desorbing pair ($0 \leqslant i \leqslant 6$, $0 \leqslant j \leqslant 8$, and $0 \leqslant i+j \leqslant 10$, Fig. 1).

Diffusion may occur whenever an adsorbate has one of its four nearest or four next-nearest neighboring sites empty, with a transition rate

$$r_{dif}^{ij} = \nu_{dif} \exp[-(\Delta + i\Delta_l + j\Delta_d)/k_B T] \tag{2a}$$

if $i\Delta_l + j\Delta_d > 0$, or

$$r_{dif}^{ij} = \nu_{dif} \exp(-\Delta/k_B T) \tag{2b}$$

if $i\Delta_l + j\Delta_d \leqslant 0$, where ν_{dif} is the diffusion pre-exponential factor, Δ is the activation energy barrier in the absence of neighbor interactions, and i and j are, respectively, the differences in the numbers of nearest and next-nearest neighbors for the adsorbate between the initial and final sites ($-3 \leqslant i \leqslant 3$, $-4 \leqslant j \leqslant 4$), following the physico-chemical argument that the energy barrier the adsorbate effectively ''sees'' when jumping onto a lower total energy site is just Δ.[16] Therefore, considering only the domain of diffusion events and understanding the term $\nu_{dif} \exp(-\Delta/k_B T)$ as a ''delay factor,'' the definitions (2) above become equivalent to the rules of the Metropolis algorithm.[17]

Within the dynamic Monte Carlo description,[6,10,12] the time evolution of the system is obtained from the microscopic transition rates as a heterogeneous Poisson process,[11] considering, for a given configuration at the instant t, the *total transition rate*

$$r_{tot} = \sum_{ij} N_{des}^{ij} r_{des}^{ij} + \sum_{ij} N_{dif}^{ij} r_{dif}^{ij}, \tag{3}$$

where N_{des}^{ij} and N_{dif}^{ij} are, respectively, the numbers (multiplicities) of the desorption and diffusion *possible events* with local environment characterized by ij. Therefore, the next event to occur is randomly chosen out of a weighted list with all the $N_{tot} = \Sigma_{ij} N_{des}^{ij} + \Sigma_{ij} N_{dif}^{ij}$ possibilities.[18] The surface lattice, the possible events' list and the multiplicities N_{des}^{ij} and N_{dif}^{ij} are then updated, and at last the time t is incremented according to

$$\tau_{inc} = (-\ln \rho) \frac{1}{r_{tot}}, \tag{4}$$

where ρ is a non-zero random number between 0 and 1.[19] The sequence of lattice configurations generated in this way is *a representative* solution for the kinetic lattice-gas model. At any instant t the system variables can be directly measured from the lattice configuration, and a better precision will be obtained by combining different runs. Particularly, we are here interested in the total number of adsorbates, N_A, and in the numbers of lateral and diagonal pairs of occupied sites, N_{AA} and N_{AA}^d, respectively, as representative functions of the local order.

Diffusion poses a serious problem to the algorithm: In real systems the surface diffusion is generally many orders of magnitude faster than desorption due to its much smaller activation energy,[14] and therefore, following all the diffusion events with physically ''realistic'' transition rates would be computationally impossible. The role of diffusion is to perform the ''redistribution'' of the adsorbates, and the fast-diffusion limit means that *the adsorbate local order shall always be in a configurational quasi-equilibrium state with respect to the desorption kinetics*.

Following the algorithm's rules, and assuming that the system is large enough to keep the multiplicities N_{des}^{ij} and N_{dif}^{ij} nearly constant, for a single desorption event there will be, on average, $\Sigma_{ij} N_{dif}^{ij} r_{dif}^{ij} / \Sigma_{ij} N_{des}^{ij} r_{des}^{ij}$ diffusion events, and thus the mean time interval for a single desorption event is[6]

$$\Delta t = \frac{1}{r_{tot}} \left[1 + \frac{\Sigma_{ij} N_{dif}^{ij} r_{dif}^{ij}}{\Sigma_{ij} N_{des}^{ij} r_{des}^{ij}} \right] = \frac{1}{\Sigma_{ij} N_{des}^{ij} r_{des}^{ij}}, \tag{5}$$

which is *independent of the diffusion velocity*, provided the N_{des}^{ij} multiplicities follow an equilibrium distribution. This allows us to look for a proper ''rescaling'' scheme to bring the r_{dif}^{ij} down to less prohibitive values, while keeping the quasi-equilibrium condition.

This was accomplished by redefining, at every event update, the term $\nu_{dif} \exp(-\Delta/k_B T)$ with respect to the possible desorption events, according to

$$\frac{\Sigma_{ij} N_{dif}^{ij} r_{dif}^{ij}}{\Sigma_{ij} N_{dif}^{ij}} = \eta \frac{\Sigma_{ij} N_{des}^{ij} r_{des}^{ij}}{\Sigma_{ij} N_{des}^{ij}}, \tag{6a}$$

where η is an arbitrary constant that defines the degree of thermalization. The invariance of the desorption kinetics will be thus attained with the choice of a sufficiently large η. A second constraint is added in that there will be a maximum mean time increment τ_{max} due to a single event,

$$r_{tot} = \sum_{ij} N_{des}^{ij} r_{des}^{ij} + \sum_{ij} N_{des}^{ij} r_{des}^{ij} \geqslant 1/\tau_{max}. \tag{6b}$$

This latter condition prevents τ_{inc} in Eq. (4) from becoming too large, which can be particularly critical in TPD simulations (Section V), where this would imply large jumps in the temperature for individual events, destroying the reliability of the simulations.

A different procedure was used by Meng and Weinberg,[4,5] where the time evolution was obtained considering just the desorption events, and treating diffusion as a thermalization process between successive desorption events. The basic advantage of our procedure presented here is that thermalization is performed as a self-adjusting process controlled by a pair of simple parameters, which shall avoid an excessive computer effort, but the overall result of the two procedures shall not be different.

For a single desorption event the change in coverage is $-2/N_s$, and combining it with Eq. (5), we have

$$\Delta\theta/\Delta t = -2\sum_{ij} (N_{des}^{ij}/N_s) r_{des}^{ij} = -4\sum_{ij} y_p^{ij} r_{des}^{ij}, \tag{7}$$

with $y_p^{ij} = N_{des}^{ij}/2N_s$, and from where we may recognize the pair desorption differential equation with local environment dependence ij.[5]

From the total number of pairs $N_{AA} = \Sigma_{ij} N_{des}^{ij}$, we may define a pair probability $y_p = \Sigma_{ij} N_{des}^{ij}/2N_s$ as the probability that two nearest neighboring sites are both occupied, and therefore it can be seen that Eq. (7) has a *direct dependence on* y_p. Indeed, in the absence of adsorbate interactions ($\Delta_l = \Delta_d = 0$) the adsorbate overlayer is randomly disordered (mean-field solution), with $y_p = \theta^2$, $r_{des}^{ij} = \nu_{des} \times \exp(-E_{des})/k_B T$), and the second-order Polanyi–Wigner differential equation[9,20] is recovered,[6]

$$\Delta\theta/\Delta t = -k_{des} \exp(-E_{des}/k_B T)\,\theta^2,$$

with $k_{des} = 4\nu_{des}$. At this point it is convenient to introduce also the next-nearest neighbor pair probability as $w_p = N_{AA}^d/2N_s$.

III. CLUSTER APPROXIMATIONS TO LOCAL ORDER AND DESORPTION KINETICS

A consistent approximation to the desorption kinetics by the Monte Carlo procedure will depend on an appropriate approximation to the partitions $\{N_{des}^{ij}\}$. These are, in reality, all the possible combinations of the numbers of nearest and next-nearest neighbors to a central nearest neighboring pair of adsorbates, resulting in sums of all the possible geometric clusters of 4×3 sites where the central sites are occupied (Fig. 1).

TABLE I. Basic and auxiliary cluster fractions used to describe the equilibrium correlation functions and desorption kinetics.

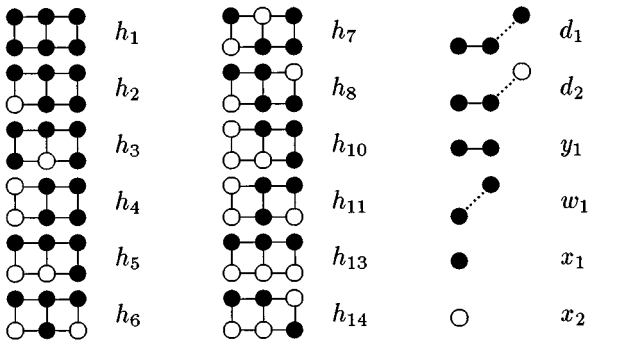

The cluster variation method (CVM), originally devised by Kikuchi,[21] is a practical method of obtaining the equilibrium properties of a lattice-gas with competing interactions in terms of a given geometric block (cluster) approximation.[22,23] The internal energy and the configurational entropy are then obtained by minimizing the resulting free energy by a self-consistent procedure.[24] The precision of the approximation will depend on the size and geometry of the basic clusters used, and the way the lattice can be built from them. The quasi-chemical[3–5,25] or Bethe[21] approximation for the square lattice is just one of the simplest cases within the CVM, but the highest order with a known analytical solution.

On testing different approximations, we have found the C_2 approximation[22] to be sufficiently precise to reproduce the both the y_p (y_1) and w_p (w_1) pair probabilities obtained by the Monte Carlo simulations in the equilibrium condition, as will be shown in the following section. All relevant cluster fractions used here and in the following sections are given in Table I; their derivation within the C_2 approximation and the specific details for the CVM calculation can be easily obtained by following the procedure described in Ref. 22 for the B_2 case.[30] The filled (●) and empty circles (○) represent, respectively, the occupied and empty surface sites.

The y_p^{ij} fractions can be estimated from the h_i-clusters by extending the combinatorial analysis of Zhdanov.[25] This is done by partitioning the 10-site immediate neighborhood of the central pair into two 4-site blocks and two 1-site blocks as shown in Fig. 1. The 4-site blocks can be filled by direct combinations of the h_i fractions that will account for the central pair, weighted by their energy contributions. On the other hand, the 1-site blocks can be filled by the d_1 and d_2 fractions (Table I). Therefore, by considering the multinomial expansion, Eq. (7) can be re-summed into

$$d\theta/dt = -4\nu_{des}\exp(-E_{des}/k_BT)y_1^{-3}h_1\exp[(3\Delta_l+3\Delta_d)/k_BT]+h_2\exp[(3\Delta_l+2\Delta_d)/k_BT]+h_2\exp[(2\Delta_l+3\Delta_d)/k_BT]$$
$$+(h_2+h_4)\exp[(2\Delta_l+2\Delta_d)/k_BT]+(h_3+h_5+h_6)\exp[(2\Delta_l+\Delta_d)/k_BT]+(h_7+h_8)\exp[(\Delta_l+2\Delta_d)/k_BT]$$
$$+(h_5+h_{10}+h_{11})\exp[(\Delta_l+\Delta_d)/k_BT]+h_{13}\exp(\Delta_l/k_BT)+h_{14}\exp(\Delta_d/k_BT)+h_{17}\}^2[d_1\exp(\Delta_l/k_BT)+d_2]^2.$$

The explicit derivation in terms of the y_p^{ij} fractions is too cumbersome to be presented here, but is not difficult to follow.

The quantitative equivalence between the numerical integrations of this last expression and the dynamic Monte Carlo simulations for TPD spectra will be shown in Section V. An approximation of higher order than C_2 could be used here in the estimation of the y_p^{ij} probabilities, but with little gain for the excess of analytical effort and numerical convergence problems involved.

IV. NUMERICAL RESULTS FOR THE PAIR PROBABILITIES: COMPARISON BETWEEN BOTH APPROACHES

Numerical results for the quasi-equilibrium nearest and next-nearest neighbors pair probabilities as function of the coverage and at fixed temperature were obtained from Monte Carlo simulations of desorption processes by recording for every single desorption interval the mean values for $N_{AA}/2N_s$ and $N_{AA}^d/2N_s$ at this coverage. The resulting data were smoothed with a Savitzky–Golay digital filter[19,26] (fourth order polynomial, window of 51 points). Throughout this section we take $\tau_{max}=\infty$, $\eta=50$, single simulations runs, $T=300$ K, but also $\nu_{des}=10^{13}$ s^{-1} and $E_{des}=1.6$ eV (the latter are, nonetheless, irrelevant here as no dynamics is concerned). There results can then be directly compared to the y_1 and w_1 pair probabilities from the C_2 approximation. For the sake of comparison, the Bethe or quasi-chemical approximation, is also presented, whenever appliable. All the computer codes used here were written in PASCAL language, and run on Sun and DEC Alpha workstations.

Figure 2(a) presents a counter-intuitive result for the nearest-neighbor pair probability y_p, with $\Delta_l=0.1$ eV and $\Delta_d=0$, exhibiting a ''dip'' at half coverage ($\theta=0.5$) where y_p falls to zero (log scale), indicating an ordering transition into a $c(2\times2)$ or ''checkerboard'' structure. This is most clearly seen in the C_2 approximation (solid line), where y_p falls to a value very close to zero at *exactly* $\theta=1/2$, increasing immediately at the left or right of this point. The latter curve is closely matched by the Monte Carlo simulation (circles), except at the region immediately left to the dip. The difference between both curves is partially due to insufficient thermalization and the finite size of the simulation, but we can infer that the C_2 approximation is not yet an exact solution to this problem. The quasi-chemical approximation (dashed line) is also plotted, presenting a *very poor* comparison to the other two curves. The next-nearest neighbor pair probability w_p is shown in Fig. 2(b) (linear scale), with an excellent comparison between the two curves, and where the ordering transition at half coverage can be recognized as a change in the derivative with respect to θ.

A much smoother transition is present when the repulsive energy is halved, as shown for y_p and w_p in Figs. 3(a) (log scale) and 3(b) (linear scale), respectively, for $\Delta_l=0.05$ eV and $\Delta_d=0$. A partial ordering transition into the $c(2\times2)$ structure is still occurring, as shown in y_p by an inflection point at half coverage in the C_2 approximation (solid line), and as a small ''depression'' around this point in the Monte Carlo simulation (circles) immediately at the left; for the rest of the graphic the curves are identical. The same is valid for w_p, with an inflection point at half coverage. The quasi-chemical approximation is also shown (dashed line), differing from the other two results in the central region.

The comparison between Figs. 2 and 3 says that the onset of an ordered $c(2\times2)$ phase should start for a given repulsion energy at this temperature. Indeed, when following the C_2 approximation over the $\theta=0.5$ line, we find that y_p falls steadily as Δ_l/k_BT is increased, as shown in Fig. 4 (the ''abrupt'' fall at $\Delta_l/k_BT\simeq3.108$ is due to round-off instabilities of the self-consistent procedure; the real curve is likely to continue according to the dashed line). This is con-

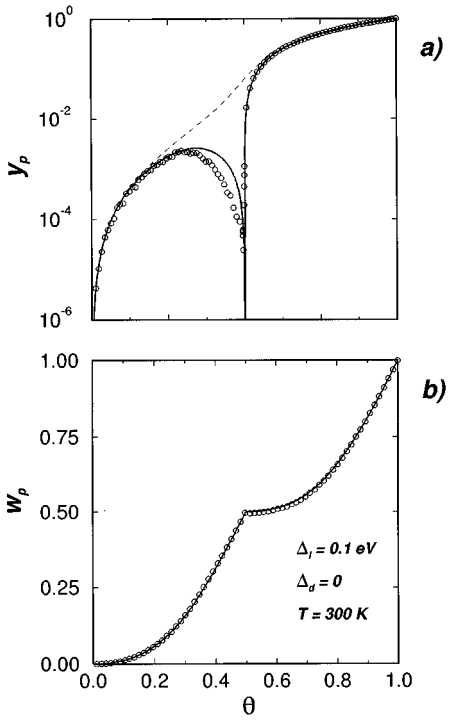

FIG. 2. Nearest and next-nearest neighbor pair probabilities y_p (a) and w_p (b) as a function of the coverage θ, for $\Delta_l=0.1$ eV and $\Delta_d=0$, at 300 K. The circles represent the simulation with $\eta=50$, the solid line is the C_2 approximation and the dashed line the quasi-chemical approximation.

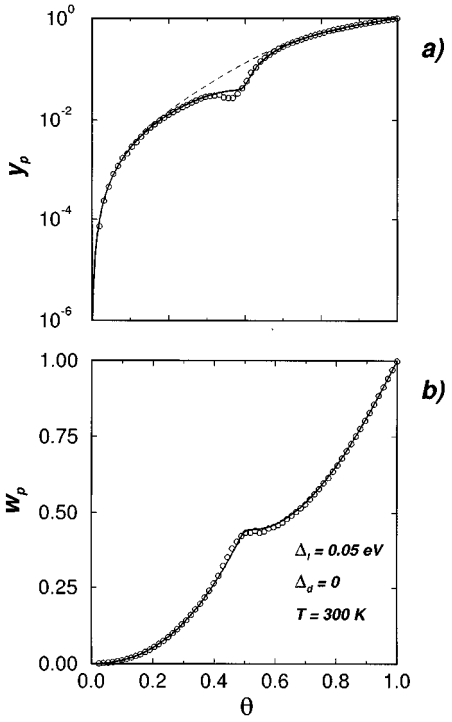

FIG. 3. The same as Fig. 2, with $\Delta_l = 0.05$ eV.

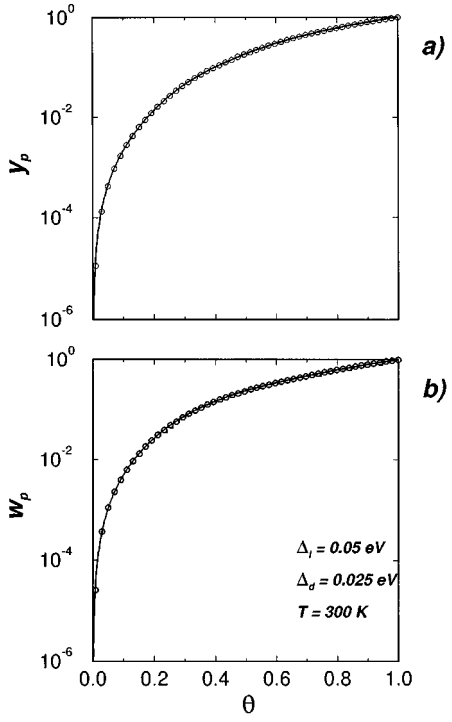

FIG. 5. The same as Figs. 2 and 3, with Δ_l 0.05 eV and Δ_d=0.025 eV.

sistent with the value $\Delta_l/k_BT \simeq 1.754$ after which the onset of the $c(2\times2)$ phase should begin (position **A** in the figure), obtained by Payne *et al.*[27] using the transfer matrix method. The ''dip'' in Fig. 2 and the ''depression'' in Fig. 3 correspond, respectively, to $\Delta_l/k_BT = 3.868$ and 1.934. Considering the Helmholtz free energy $F=E-TS$, the ordering transition is thus a situation where a minimum internal energy E can be attained at the expense of a minimum entropy S. This phase transition will thus explain the results of Cao,[28] who obtained strong variations in the diffusion coefficient of a lattice-gas around half coverage as the nearest-neighbor repulsion energy was varied. This ordering effect also occurs due to the absence of a next-nearest neighbor repulsion term. With its inclusion, competition between both repulsions will arise and the ''checkerboard'' order will be destroyed. However, a compromise between the internal energy and the configuration entropy will always exist for the minimum free energy,[27,29] and thus a lowering of y_p can always be found for appropriate energy parameters.

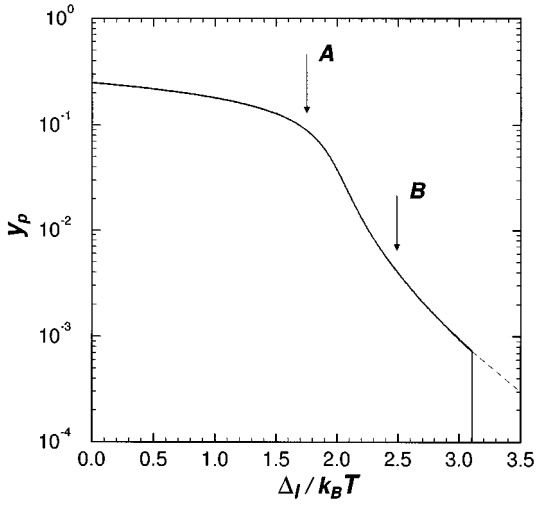

FIG. 4. Nearest-neighbor pair probability y_p as a function of the reduced energy Δ_l/k_BT at $\theta = 0.5$ within the C_2 approximation. The dashed line is the probable continuation of the curve, which falls to zero due to round-off errors. Position **A** is the point after which the onset of the $c(2\times2)$ phase takes place according to Payne *et al.* (Ref. 27), and position **B** corresponds to the desorption minimum of Fig. 6 with $\theta_0=1$.

A simpler case without the presence of the ordering transition is shown in Fig. 5, with $\Delta_l=0.1$ eV and $\Delta_d=\Delta_l/2$, within a dipole dependence of the repulsive potential. A very good comparison is found between the simulation (circles) and the CVM calculation (solid line) for either y_p or w_p.

This last set of figures shows that the quasi-equilibrium local order obtained by the Monte Carlo simulation can be very well approximated by the C_2 approximation, except in the regions immediately left to $\theta=0.5$ in Figs. 2 and 3, where a partial ordering transition is occurring, and we may infer that this approximation is yet ''incomplete,'' even though sufficient for our purposes.[30] A higher-order approximation could be used here, but this would imply difficulties in the self-consistent numerical convergence due to a much larger number of independent variables.

The equivalence should not be surprising, however, if we recognize the diffusion rates (2) as equivalent to the Metropolis algorithm,[17] which was devised as a method for *simulating* the equation of state for a given Hamiltonian. On the other hand, the CVM is an *explicit* calculation of an equation of state of a lattice-gas system, and thus *an equiva-*

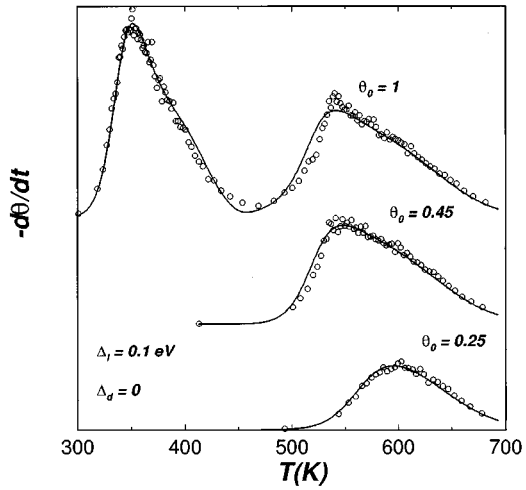

FIG. 6. TPD spectra for $T_0=300$, $\beta=4$ K/s, $\nu_{des}=10^{13}$ s^{-1}, $E_{des}=1.6$ eV, $\Delta_l=0.1$ eV, and $\Delta_d=0$, for initial coverages $\theta_0=1$, 0.45 and 0.25. Simulation runs are represented by circles ($\tau_{max}=0.1$ s and $\eta=50$) and cluster approximations by solid lines.

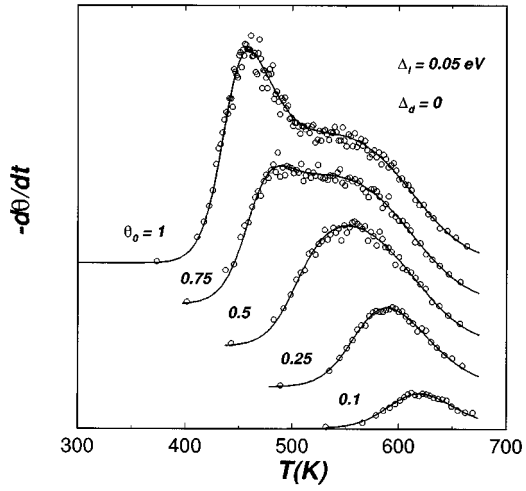

FIG. 7. The same as Fig. 6, with $\Delta_l=0.05$ eV and $\theta_0=1$, 0.75, 0.5, 0.25, and 0.1.

lence can be achieved if a suitable approximation is used within the CVM, as we found with C_2.

Finally, Figs. 2(a) and 3(a) show clearly that the quasichemical approximation fails drastically in describing the local order when a single interaction energy is concerned, except for the extremes at the high and low coverages far from the ordering regions, and therefore severely limiting its applicability to problems in reaction and desorption kinetics.[3–5,31]

V. TEMPERATURE-PROGRAMMED DESORPTION SPECTRA

In the temperature-programmed desorption (TPD) the time derivative of the surface coverage is recorded as a function of the temperature, that is also as a ''programmed'' function of the time, usually[9,20,32]

$$T=T_0+\beta t, \tag{8}$$

where T_0 is the initial temperature and β the temperature advancement rate, with adsorption proceeding from an initial coverage θ_0. A TPD spectrum is thus a ''collective signature'' of all the simultaneous events of desorption and diffusion, as function of the experimental parameters θ_0, T_0 and β.

In the dynamic Monte Carlo simulations of TPD processes, the system was initialized by randomly filling $\theta_0 N_s$ sites of the square lattice and letting it thermalize through $\eta\Sigma_{ij}N_{dif}^{ij}$ diffusion steps. Thereafter, after each succeeded event, t and T are increased according to Eqs. (4) and (9), respectively, and after each desorption event the current values of θ, t, T, y_p and w_p are recorded. The final results were taken as the average of 10 independent runs, and the time derivative of θ and absolute values above were smoothed with the Savitzky–Golay filter.[19,26]

The simulations are compared to the integration of Eqs. (8) and (9) with a fourth-order Runge–Kutta procedure, using an adaptive size step scheme[19] where, at each integration step the h_i, d_i and y_1 fractions are obtained self-consistently by the C_2 calculation for the current values of $x_1\equiv\theta$ and T.

Throughout this section we used $\nu_{des}=10^{13}$ s^{-1}, $E_{des}=1.6$ eV, $T_0=300$ K and $\beta=5$ K/s, and in the simulations, $\eta=50$ and $\tau_{max}=0.1$ s. The TPD spectra corresponding to the energy parameters of Fig. 2, $\Delta_l=0.1$ eV and $\Delta_d=0$, are shown if Fig. 6, with $\theta_0=1$, 0.45 and 0.25 (top to bottom). The circles represent the Monte Carlo simulations, and the solid lines the cluster approximation. The $\theta_0=1$ spectrum is split into two at half coverage with $T\simeq 465$ K, corresponding to the onset of the $c(2\times2)$ phase, with $\Delta_l/k_BT\simeq 2.496$ and $y_p\simeq 4.18\times10^{-3}$ (point **B** in Fig. 4), where desorption virtually stops due to the almost absolute absence of desorption pairs. Then, as temperature increases, the $c(2\times2)$ phase is overcome, and desorption is resumed (a similar path over the phase diagram is found for non-recombinative desorption[3]). There is a good correspondence between simulation and cluster approximation curves, except for the region around and immediately below half coverage, where the correspondence in the quasi-equilibrium is incomplete, as seen in Figs. 2 and 3. A much better correspondence is thus found for the $\theta_0=0.45$ and 0.25 pairs of curves.

This last result shows precisely how an order-disorder transition may show itself in TPD spectra. Multiple peaks in desorption spectra have since long been known[15,33] to arise from adsorbate-adsorbate interactions, but their relation to the ordered phases was only possible with either Monte Carlo[3] or approximate[27] solutions to lattice-gas models. The relation to the ordered phases is enhanced here if we consider a conceptual difference between recombinative and non-recombinative desorption kinetics: In the recombinative case the total desorption rate depends *directly on the total number of pairs available to desorption*, $N_{AA}=\Sigma_{ij}N_{des}^{ij}$ with an ''envelope'' dependence, and not just on their distribution among the N_{des}^{ij} multiplicities and the associated r_{des}^{ij} arising from the interactions. Ordered structures are well known to

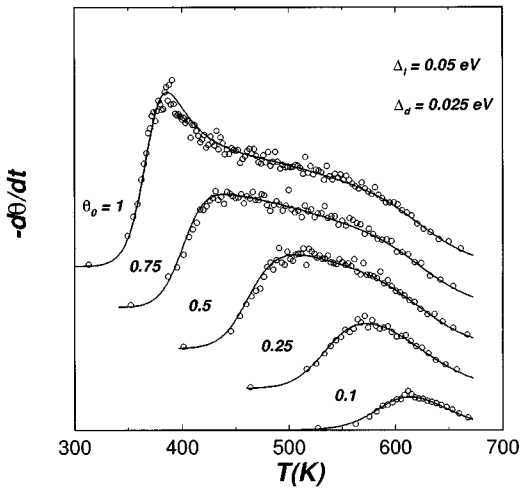

FIG. 8. The same as Figs. 6 and 7, with $\Delta_l=0.05$ eV, $\Delta_d=0.025$ eV, for $\theta_0=1$, 0.75, 0.5, 0.25, and 0.1.

be formed by chemisorbed hydrogen around half coverage and low temperatures on low-index planes of metals like Ni, Co and Pd.[34] Therefore, a situation similar to Fig. 6 would occur with the observed β_1 and β_2 features of TPD spectra for H_2 from Ni and Co[35] and W(100).[20]

A much better correspondence between the Monte Carlo simulations and the cluster approximations is shown in Fig. 7 and 8 for the energy parameters of Figs. 3, $\Delta_l=0.05$ eV and $\Delta_d=0$, and 5, $\Delta_l=0.05$ eV and $\Delta_d=0.025$ eV, respectively, for $\theta_0=1$, 0.75, 0.5, 0.25 and 0.1 (top to bottom). A more ''conventional'' peak broadening can be recognized as a continuous overlap due to the different activation energies arising from the interactions. The slight differences in the latter figure should be due to yet incomplete approximation of the y_p^{ij} terms by the h_i clusters in Eq. (7) when too large repulsions are present.

VI. CONCLUSIONS AND FINAL REMARKS

The dynamic Monte Carlo method was applied to the simulation of temperature-programmed desorption processes of a diatomic species dissociatively adsorbed on a metallic surface represented by a square lattice, considering the local processes of pair desorption and surface diffusion with local dependencies due to both nearest (lateral) and next-nearest neighbor (diagonal) interactions between the adsorbates, in the limit of fast diffusion with respect to desorption. The last condition ensures that the adsorbate layer is in a quasi-equilibrium state, so that the desorption kinetics can be shown to have a direct dependence on the equilibrium local order induced by the interactions between the adsorbates. Therefore, the desorption kinetics obtained from the Monte Carlo procedure can be ''reproduced'' with the use of a statistical approximation that describes properly the local order. This was achieved with the C_2 approximation of the cluster variation method, allowing a very good quantitative reproduction to both dynamical desorption spectra and equilibrium pair correlation functions resulting from the simulation.

The quantitative agreement between the two approaches thus has two immediate implications:

(i) it is shown that the dynamic Monte Carlo algorithm does indeed provide the correct time evolution of the stochastic system, even when a continuous step-by-step rescaling of one process with respect to another is included;

(ii) the Monte Carlo simulation can be successfully substituted by a differential equation formalism provided the system's kinetics depends directly on a quasi-equilibrium condition that can be appropriately described.

These two points deserve a further few comments: the temperature-programmed desorption simulations presented here are a *tour de force* for the dynamic Monte Carlo method, since they comprise two classes of different, but interrelated, basic processes (diffusion and desorption) with transition rates that are also a direct function of the time. Monte Carlo simulations are, however, rather expensive in terms of computer effort and bear inaccuracies due to statistical noise that can be just partially smoothed out by either the combination of different runs or with the use of digital filters. The cluster approximations, on the other hand, are much faster calculations with smooth results, but as it is found with the C_2 case, they may be incomplete in some cases, or become rather complicated as the number of variables increases with the order of the approximation, leading also to numerical convergence problems. This can be, in turn, a point of advantage for the Monte Carlo methods, for they can always be defined in terms of a simple set of probabilistic rules.

A careful weighing of the two approaches should be made when extending this simple model of desorption plus diffusion with immediate neighborhood interactions onto more realistic problems. Thus, even though this model is able to describe a wide range of experimental results, it has to be extended to include basic processes like adsorption, precursor states, surface reconstructions, heterogeneity in the chemisorption sites, etc., or even more complex situations of catalytic surface reactions, like $CO+1/2\,CO_2 \rightleftharpoons CO_2$ over Pd or Pt.[36] Therefore, even in the situation where a quasi-equilibrium condition can be applied, finding out an appropriate equilibrium configuration may not always be a feasible task. Nevertheless, a combination of both methods can be pursued in some situations (see Table II).

ACKNOWLEDGMENTS

S.W. acknowledges financial support from the Coordenação de Aperfeiçoamento de Pessoal de Nível Superior—CAPES and the Fundo de Apoio ao Ensino e Pesquisa—FAEP (UNICAMP), and G.G.C. acknowledges partial support from the Conselho Nacional de Desenvolvimento Científico e Tecnológico—CNPq. The authors also acknowledge important remarks from Hannibal H. Madden, Jr., and A. L. Cabrera.

[1] E. S. Hood, B. H. Toby, and W. H. Weinberg, Phys. Rev. Lett. **55**, 2437 (1985).
[2] (a) J. L. Sales and G. Zgrablich, Phys. Rev. B **35**, 9520 (1987); (b) Surf. Sci. **187**, 1 (1987); (c) S. J. Lombardo and A. T. Bell, *ibid.* **206**, 101 (1988); (d) D. Gupta and C. S. Hirtzel, *ibid.* **210**, 322 (1989); (e) L. V. Lutsevich, O. A. Tkatchenko, and V. P. Zhdanov, Langmuir **7**, 1225 (1991); (f) **8**, 1757 (1992); (g) A. P. J. Jansen, Comput. Phys. Commun. **86**, 1 (1995).
[3] J. L. Sales, G. Zgrablich, and V. P. Zhdanov, Surf. Sci. **209**, 208 (1989).
[4] B. Meng and W. H. Weinberg, J. Chem. Phys. **100**, 5280 (1994).
[5] B. Meng and W. H. Weinberg, J. Chem. Phys. **102**, 1003 (1995).
[6] S. Weinketz, J. Chem. Phys. **101**, 1632 (1994).
[7] (a) H. J. Kreuzer, Appl. Phys. A **51**, 491 (1990); (b) H. J. Kreuzer and J. Zhang, *ibid.* **51**, 183 (1990); (c) H. J. Kreuzer, Langmuir **8**, 774 (1992).
[8] L. D. Schmidt, in *Interactions on Metal Surfaces*, Topics in Applied Physics, Vol. 36, edited by R. Gomer (Springer, New York, 1975).
[9] R. P. H. Gasser, *An Introduction to Chemisorption and Catalysis by Metals* (Oxford University Press, Oxford, 1987).
[10] K. A. Fichthorn and W. H. Weinberg, J. Chem. Phys. **95**, 1090 (1991).
[11] B. E. Cooper, *Statistics for Experimentalists* (Pergamon, Oxford, 1969).
[12] (a) D. T. Gillespie, J. Comput. Phys. **22**, 403 (1976); (b) J. Phys. Chem. **81**, 2340 (1977).
[13] S. M. George, A. M. DeSantolo, and R. B. Hall, Surf. Sci. Lett. **159**, L425 (1985).
[14] R. Gomer, Rep. Prog. Phys. **53**, 917 (1990).
[15] D. L. Adams, Surf. Sci. **42**, 12 (1974).
[16] K. J. Laidler, *Chemical Kinetics*, 3rd ed. (Harper and Row, New York, 1987).
[17] N. Metropolis, A. W. Rosenbluth, M. N. Rosenbluth, A. H. Teller, and E. Teller, J. Chem. Phys. **21**, 1087 (1953).
[18] A. B. Bortz, M. H. Kalos, and J. L. Lebowitz, J. Comput. Phys. **17**, 10 (1975).
[19] W. H. Press, S. A. Teukolsky, W. T. Vetterling, and B. P. Flannery, *Numerical Recipes in FORTRAN: The Art of Scientific Computing*, 2nd ed. (Cambridge University Press, Cambridge, 1992).
[20] D. Menzel, in Ref. 8.
[21] R. Kikuchi, Phys. Rev. **81**, 988 (1951).
[22] R. Kikuchi and S. G. Brush, J. Chem. Phys. **47**, 195 (1967).
[23] D. de Fontaine, *Configurational Thermodynamics of Solid Solutions*, *Solid State Physics* (Academic, New York, 1979).
[24] R. Kikuchi, J. Chem. Phys. **60**, 1071 (1974).
[25] V. P. Zhdanov, Surf. Sci. Lett. **102**, L35 (1981).
[26] H. H. Madden, Jr., Anal. Chem. **50**, 1383 (1978).
[27] S. H. Payne, H. J. Kreuzer, and L. D. Roelofs, Surf. Sci. Lett. **259**, L781 (1991).
[28] P. L. Cao, Phys. Rev. Lett. **73**, 2595 (1994).
[29] K. Binder and D. P. Landau, Surf. Sci. **108**, 503 (1981).
[30] The B_2 approximation (Ref. 22) gives very similar results to the C_2 approximation in Figs. 2 and 3, reproducing both y_p and w_p, although it is slightly worse in the region immediately left to $\theta=0.5$, which is also an indication that none of the two is ''exact'' with respect to the Monte Carlo simulations. The B_2 approximation, however, fails drastically when any diagonal interaction term, $\Delta_d > 0$, is included.
[31] (a) J. R. Smith, Jr. and A. Zangwill, Surf. Sci. **316**, 359 (1994); (b) A. Datar and S. D. Prasad, J. Chem. Phys. **100**, 1742 (1994).
[32] P. A. Redhead, Vacuum **12**, 203 (1962).
[33] Reference 20, p. 115.
[34] K. Christmann, Ber. Bunsenges. Phys. Chem. **90**, 307 (1986).
[35] (a) A. L. Cabrera, J. Vac. Sci. Technol. A **8**, 3229 (1990); (b) **11**, 205 (1993).
[36] (a) J. Szanyi, W. K. Kuhn, and D. W. Goodman, J. Vac. Sci. Technol. A **11**, 1969 (1993); (b) J. Szanyi and D. W. Goodman, J. Phys. Chem. **98**, 2972 (1994).